Available online at www.sciencedirect.com
ScienceDirect
Journal of Power Sources 169 (2007) 253–258
JOURNAL OF POWER SOURCES
www.elsevier.com/locate/jpowsour

Short communication

Ni/YSZ and Ni–CeO_2/YSZ anodes prepared by impregnation for solid oxide fuel cells

Jinshuo Qiao [a,1], Kening Sun [a,*], Naiqing Zhang [a,b,1], Bing Sun [a,1], Jiangrong Kong [a,1], Derui Zhou [a,1]

[a] *Department of Applied Chemistry, Harbin Institute of Technology, No. 92, West Da-Zhi Street, Box 211, Harbin, Heilongjiang 150001, PR China*
[b] *The Research Station on Material Science and Engineering for Postural Fellows, Harbin Institute of Technology, No. 92, West Da-Zhi Street, Box 211, Harbin, Heilongjiang 150001, PR China*

Received 6 January 2007; received in revised form 4 March 2007; accepted 5 March 2007
Available online 5 April 2007

Abstract

In this paper, Ni/YSZ and Ni–CeO_2/YSZ anodes for a solid oxide fuel cell (SOFC) were prepared by tape casting and vacuum impregnation. By this method, the Ni content in the anode could be reduced compared to the traditional tape casting method. It was found that adding CeO_2 into the Ni/YSZ anode by a $Ni(NO_3)_2$ and $Ce(NO_3)_3$ mixed impregnation could further enhance cell performance. This was investigated in H_2 at 1073 K. XRD patterns indicated that CeO_2 and Ni were separate phases, and the CeO_2 addition could enhance the Ni dispersion on the YSZ framework surface which was observed by SEM images. It was shown that adding CeO_2 into the Ni anodes could decrease the cell polarization resistance. The maximum power density for cells with 25 wt.% Ni, 5 wt.% CeO_2–25 wt.% Ni/YSZ, or 10 wt.% CeO_2–25 wt.% Ni/YSZ anode was 230 mW cm^{-2}, 420 mW cm^{-2} and 530 mW cm^{-2}, respectively, in H_2 at 1073 K. The OCV for these cells was 1.05–1.09 V, indicating that a dense electrolyte film was obtained by co-firing porous YSZ layer and dense YSZ layer.

Keywords: Solid oxide fuel cell (SOFC); Ni–CeO_2–YSZ anode; Tape casting; Vacuum impregnation

1. Introduction

Solid oxide fuel cells (SOFCs) are anticipated to be viable sources for power generation in the future due to high efficiency, high waste-heat utilization and low emission of pollutants [1]. At present, low- and intermediate-temperature SOFCs are widely studied [2–5]. Ni/YSZ anode supported SOFCs using YSZ electrolyte film are still being developed because of the advantages of low cost and easy manufacturability. Commonly, the Ni/YSZ anode is prepared by tape casting or by uniaxial pressure. The YSZ electrolyte is fabricated by co-tape casting or screen-printing and the electrolyte/anode composite is co-fired above 1723 K [6,7]. Anode performance is affected because of the agglomeration of Ni at high temperature. On the other hand, a high Ni content in the traditional Ni/YSZ anode easily leads to cracks or warps of the electrolyte/anode composite during co-firing because of the different thermal expansion coefficients [8]. Thus, reducing the sintering temperature or decreasing the Ni content in the anode is desirable. Nano-YSZ powder can be used to fabricate the electrolyte, and the co-sintering temperature can be reduced to 1673 K [9].

In this work, Ni/YSZ anodes were prepared by a vacuum impregnation method in order to reduce the Ni content. Similar work was reported by Gorte et al. [10–12], but their interest was focused on the Cu-based anode for the direct oxidation of hydrocarbon due to the low melting point of copper. CeO_2 was added into the Ni/YSZ anode by a $Ni(NO_3)_2$ and $Ce(NO_3)_3$ mixture to enhance anode performance, and the influence of CeO_2 on the Ni/YSZ anode was studied in detail. As-fabricated anodes were compared with traditional Ni/YSZ anodes prepared by tape casting and co-firing methods.

* Corresponding author. Tel.: +86 451 8641 2153; fax: +86 451 8641 2153.
E-mail addresses: qjs_1980@163.com (J. Qiao), sunkn@hit.edu.cn, sunkn_skn@yahoo.com.cn (K. Sun), znqzjz@sohu.com.cn (N. Zhang), mujuhit@126.com (B. Sun), helendino@163.com (J. Kong), zhou@hope.hit.edu.cn (D. Zhou).
[1] Tel.: +86 451 8641 2153; fax: +86 451 8641 2153.

0378-7753/$ – see front matter © 2007 Elsevier B.V. All rights reserved.
doi:10.1016/j.jpowsour.2007.03.006

2. Experimental

The cells were fabricated as follows. Firstly, the YSZ wafer was cut from green tapes produced by casting a YSZ (China, 8 mol% Y_2O_3) layer containing starch pore formers onto a thin YSZ electrolyte layer containing no pore formers. This tape was fired at 1773 K for 6 h, and the p-YSZ/d-YSZ substrate containing 60–65 vol.% porosity was measured by Archimedes method. The thin YSZ electrolyte layer formed a dense-YSZ (d-YSZ) film of about 30 μm thickness. The porous-YSZ (p-YSZ) layer was ~800 μm in thickness to form the anode. Secondly, the porous anode layer was impregnated with an aqueous solution of $Ni(NO_3)\cdot 6H_2O$ (99.9%) or $Ni(NO_3)\cdot 6H_2O$ (99.9%) and $Ce(NO_3)\cdot 6H_2O$ (99.9%) under vacuum condition, then calcined to 1073 K to decompose the nitrate ions and form NiO or NiO–CeO_2. Contents of Ni or CeO_2 in the anodes were controlled by the impregnation steps. This method was called tape casting impregnation (TCI). Finally, a 0.5 cm^2 cathode was applied by painting a Pt paste onto the exposed surface of the YSZ electrolyte follow by calcination in air at 1123 K for 1 h.

The NiO–YSZ/YSZ composite ceramic was prepared by tape casting and co-firing—the TCC method [13]. The anodes contained 56 wt.% NiO (Sinopharm Chemical Reagent, 99.9%). The sintering process was at 1773 K for 6 h in air. The same Pt cathode was burned on the YSZ electrolyte.

Ag wires were adhered to the cathode and anode by Ag paste as the current collectors. The cell was assembled in a zirconia tube with a glass–ceramic sealant and placed in a furnace (see in Fig. 1). The discharge performance of cells was measured by Arbin instruments, using 60 sccm flow rate H_2 fuel with a humidity of approximately 3% for anode at 1073 K. The cathode was exposed to air. Electrochemical impedance spectra (EIS) were collected using M2273 advanced electrochemical system (Parstat) for the frequency range of 0.05 Hz–100 kHz at the open circuit condition. Scanning electron microscopy (SEM) was used to observe the anode microstructure with a Hitachi S4700. The phases present within the anodes after exposure to H_2 conditions for 1 h, were determined with X-ray diffraction (XRD) using Cu Kα radiation.

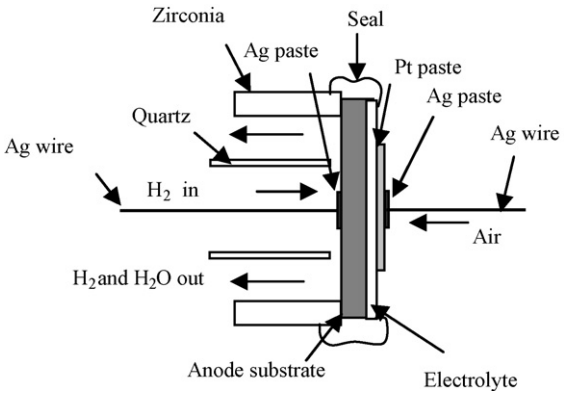

Fig. 1. Schematic of a SOFC test system.

3. Results and discussion

3.1. Cell performance with different Ni content anodes prepared by the TCI method

Micrographs of the surface of p-YSZ and the cross-sections of p-YSZ/d-YSZ are shown in Fig. 2. A continuous porous YSZ framework was formed and the thin YSZ film was ~30 μm (Fig. 2a and b). Ni/YSZ anodes with different Ni contents were estimated through the discharge curves in H_2 at 1073 K (Figs. 3 and 4). In Fig. 3, a p-YSZ/d-YSZ sub-

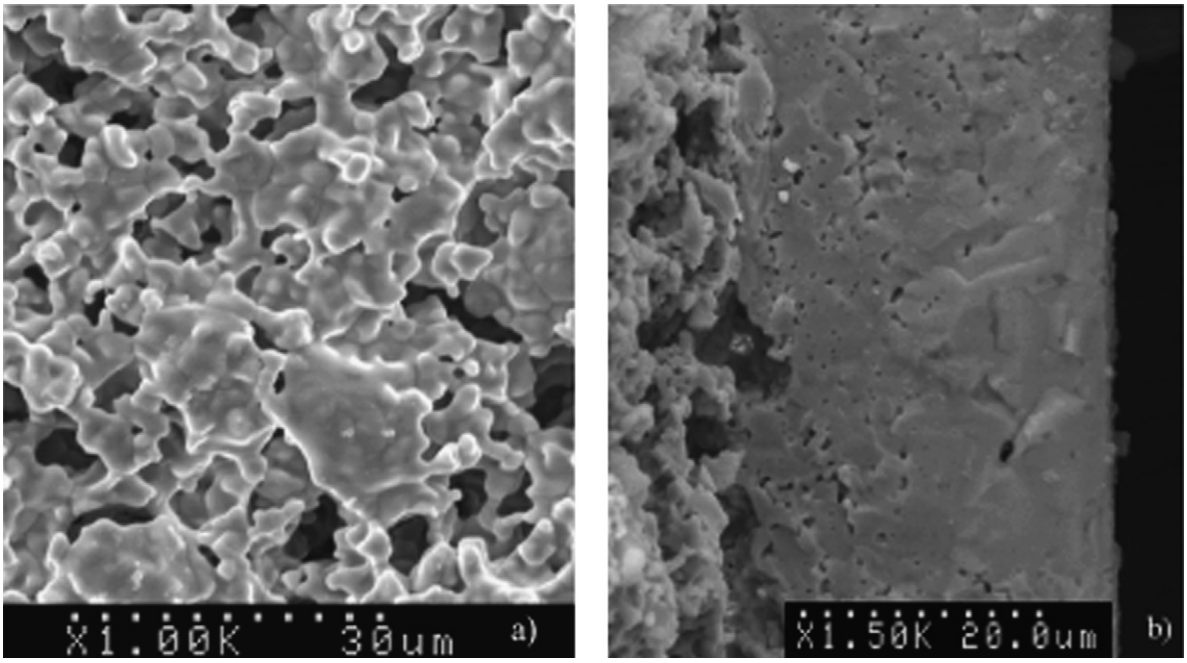

Fig. 2. SEM graphs of p-YSZ/d-YSZ: (a) p-YSZ surface and (b) cross-section for p-YSZ/d-YSZ.

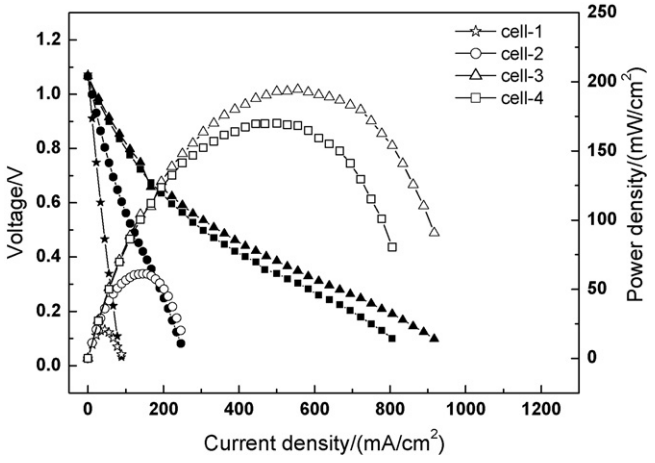

Fig. 3. Power densities and current densities-voltage relationships for SOFC unit cells with different Ni content anodes at 1073 K in H_2 (cell-1: 16 wt.% Ni; cell-2: 20 wt.% Ni; cell-3:25 wt.%Ni; cell-4: 30 wt.% Ni).

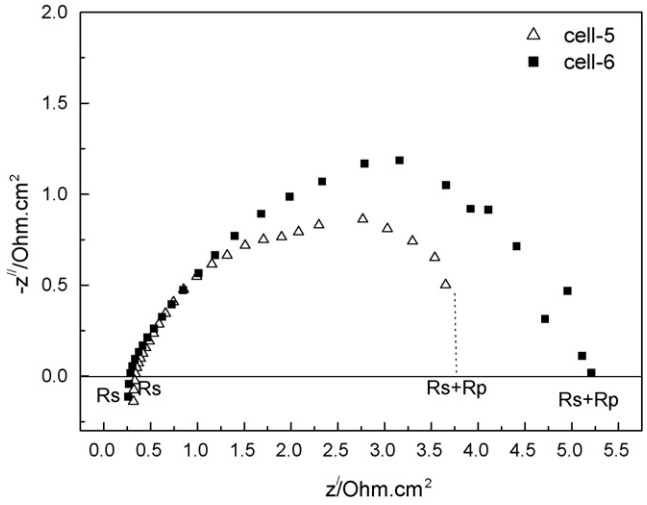

Fig. 5. Impedance spectra obtained with cell-5 and cell-6 in H_2 at 1073 K.

strate with ~60 vol.% porosity was immersed in $Ni(NO_3)_2$ to obtain the Ni/YSZ anodes. The power densities of cell-2 and cell-3 increased from 61 mW cm^{-2} to 194 mW cm^{-2} when the impregnated Ni content increased from 20 wt.% to 25 wt.%. This could be attributed to the increase of nickel leading to higher conductivity, and the ohmic resistance for cell-2 and cell-3 was 0.757 Ω cm^2 and 0.270 Ω cm^2, respectively. When the Ni content was 30 wt.% for cell-4, the ohmic resistance was 0.204 Ω cm^2. The ohmic resistance decreased further, but the power density of cell-4 was 170 mW cm^{-2}—lower than cell-3. Cell-5 and cell-6 were prepared, with Ni contents of 25 wt.% and 30 wt.%, respectively. Similar results were obtained for cell-5 and cell-6, as shown in Fig. 4. The power density of cell-6 was 230 mW cm^{-2} and slightly lower than cell-5. Electrochemical Impedance spectra obtained for cell-5 and cell-6 are shown in Fig. 5. The ohmic resistance (R_s) corresponds to the intercept of the impedance with the real axis at high frequencies, which includes electrolyte resistance, the electrode material resistance, and the contact resistance due to non-optimized contact and current collection. The impedance spectra arcs represent the polarization resistance (R_p) of the unit cells correlate with the electrochemical reactions. The R_s for cell-5 and cell-6 is 0.275 Ω cm^2 and 0.215 Ω cm^2, respectively. This also showed increasing Ni content could reduce cell ohmic resistance. But R_p for cell-5 is smaller than that of cell-6s, the resistance value was 4.092 Ω cm^2 for cell-5 and 5.344 Ω cm^2 for cell-6. This indicated that a 30 wt.% Ni content was slightly too high for anodes prepared by the impregnation method. It is possible that the reduced Ni from NiO on the YSZ surface partially agglomerated, which led to the decrease of the triple-phase boundary region and an increase in the cell polarization resistance. This result is consistent with the discharge performance of these two cells shown in Fig. 4. In the following section, we studied the Ni anode performance with CeO_2 additions.

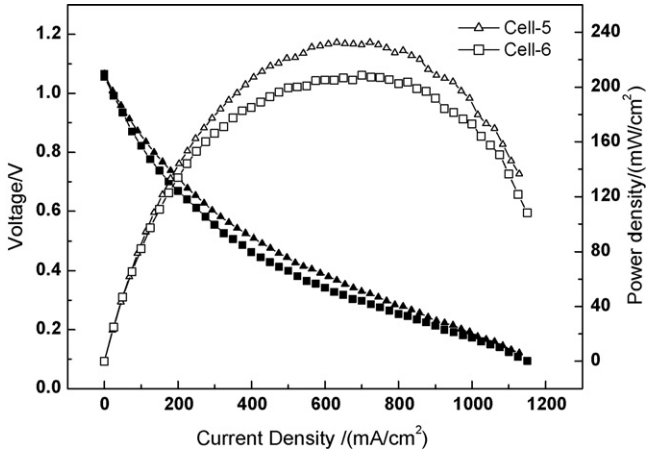

Fig. 4. Power densities and current densities–voltage relationships for cell-5 and -6 at 1073 K in H_2 (cell-5: 25 wt.% Ni; cell-6: 30 wt.% Ni).

The differentiation of cell-5 and cell-6 from cell-3 and cell-4 is that the p-YSZ/d-YSZ substrates used to prepare their anodes were of different porosity. The p-YSZ/d-YSZ substrate porosity for cell-5 and cell-6, was 65 vol.%, and for cell-3 and cell-4 was 60 vol.%. The maximum power densities for cell-5 and cell-6 were 232 mW cm^{-2} and 207 mW cm^{-2} and higher than those of cell-3s and cell-4s, indicating that porosity of p-YSZ substrate could also affect the performance of cells. A large porosity was useful for enhancing cell performance.

3.2. *Effect of adding CeO_2 on anode performance*

Ni–CeO_2/YSZ anodes with different ratios of Ni to CeO_2 were prepared by immersing in mixed solutions of $Ni(NO_3)$ and $Ce(NO_3)$. The porosity of the p-YSZ/d-YSZ substrate was 65 vol.% before impregnation. The discharge curves of these cells at 1073 K with H_2 as fuels are shown in Fig. 6. From Figs. 4 and 6, doping CeO_2 in NiO/YSZ anode could enhance the cell performance at some extent. The maximum power density for cell-7 with 3 wt.% CeO_2–27 wt.% Ni/YSZ anode and cell-8 with 5 wt.% CeO_2–25 wt.% Ni/YSZ were 315 mW cm^{-2} and 420 mW cm^{-2}, respectively. The maximum power densities of cells decreased when Ni was decreased to under the 30 wt.%. This result can be attributed to the increase of R_s of these cells,

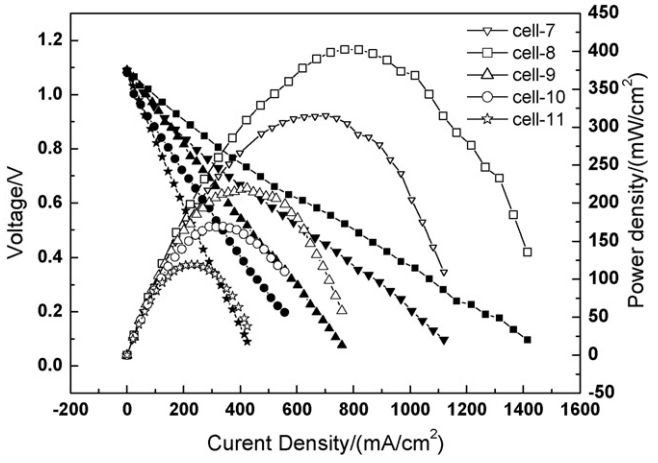

Fig. 6. Power densities and current densities–voltage relationships for SOFC using a 30 wt.% Ni–CeO_2 anode at 1073 K, and the ratio of Ni:CeO_2 was different. (Cell-7: 3 wt.% CeO_2–27 wt.% Ni; cell-8: 5 wt.% CeO_2–25 wt.% Ni; cell-9: 10 wt.% CeO_2–20 wt.% Ni; cell-10: 12 wt.% CeO_2–18 wt.% Ni; cell-11: 15 wt.% CeO_2–15 wt.% Ni.)

which was demonstrated by the impedance spectra for cell-7, cell-8, cell-9 and cell-11 as shown in Fig. 7. Figs. 7 and 5 which show the total resistance for each unit cell. It is difficult to clearly distinguish the cathode and anode process. All unit cells in this study had the same cathode and electrical contacts to the electrodes. The difference between unit cells is due to the anode performance difference. The R_s, R_p values and the maximum power densities for cell-5, cell-6, cell-7, cell-8, cell-9 and cell-11 are given in Table 1.

The R_s for cell-8 is slightly smaller than that of the cell-5s with 25 wt.% Ni in SOFC anode. This could be explained by the actual Ni content increase for 5 wt.% CeO_2–25 wt.% Ni anode. The R_s for cell-9 and cell-11 is 0.71 Ω cm^2 and 0.70 Ω cm^2, respectively, which is higher than that of cell-8. The R_s increase of cell-9 and cell-11 could be explained by an anode ohmic resistance increase due to the Ni content decrease in the SOFC anode. On the other hand, doping with CeO_2 in the Ni anode reduced the polarization resistance (R_p) of the unit cells. The R_p

Table 1
R_s, R_p values and maximum power densities for cell-5, cell-6, cell-7, cell-8, cell-9 and cell-11

	Cells name					
	Cell-5	Cell-6	Cell-7	Cell-8	Cell-9	Cell-11
R_s (Ω cm^2)	0.275	0.215	0.217	0.22	0.71	0.70
R_p (Ω cm^2)	4.09	5.344	1.321	0.89	0.98	1.21
P_{max} (mW cm^{-2})	232	207	315	420	219	119

Cell-5: 25 wt.% Ni; cell-6: 30 wt.% Ni; cell-7: 27 wt.% Ni–3 wt.% CeO_2; cell-8: 25 wt.% Ni–5 wt.% CeO_2; cell-9: 20 wt.% Ni–10 wt.% CeO_2; cell-11: 15 wt.% Ni–15 wt.% CeO_2.

for cell-7, cell-8, cell-9 and cell-11 was far lower than the R_p for cell-5 and cell-6. Thus, it can be seen that CeO_2 addition is favorable for the H_2 reaction on the electrode. The reason is that CeO_2 is helpful for H_2 adsorption and dissociation on the Ni particle surface. At the same time, adding CeO_2 enhanced the Ni dispersion on the surface of the YSZ framework to prevent Ni sintering during the reaction. For the cell with Ni–CeO_2 anode, the R_p was altered with 1.32 Ω cm^2 for cell-7, 0.89 Ω cm^2 for cell-8, 0.99 Ω cm^2 for cell-9 and 1.21 Ω cm^2 for cell-11. The R_p increase could be attributed to a triple-phase boundary region reduction because of the Ni content decrease in the SOFC anode.

Cell-12 with a 10 wt.% CeO_2–25 wt.% Ni/YSZ anode was prepared by the same method as cell-7, cell-8, cell-9, cell-10 and cell-11, which was estimated in H_2 at 1073 K (Fig. 8). The maximum power density for cell-12 was up to 530 mW cm^{-2} and higher than that of cell-8 at 1073 K. Impendence spectra from Fig. 9 show that the R_p for cell-12 is 0.79 Ω cm^2 and is further reduced compared with cell-8. XRD patterns of the anode compositions after reduction at 1073 K for 1 h are shown in Fig. 10. Ni diffraction peaks weakened as the CeO_2 content increased in the Ni/YSZ anodes. Ni and CeO_2 were separate phases. Adding CeO_2 into Ni/YSZ by mixed-impregnation of $Ni(NO_3)$ and $Ce(NO_3)$ solutions improved the Ni dispersion on the YSZ surface and enhanced the anode activity. Fig. 11a shows the SEM images for the surface Ni–CeO_2/YSZ after reaction with H_2. Ni–CeO_2 is still uniformly dispersed on the YSZ

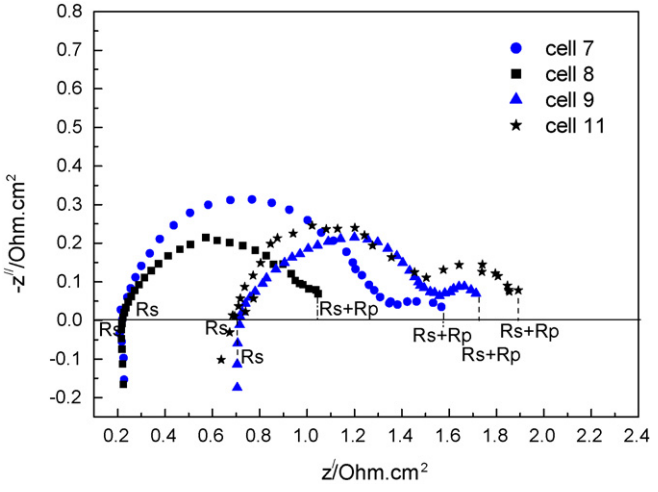

Fig. 7. Impedance spectra obtained with cell-7, cell-8, cell-9 and cell-11 in H_2 at 1073 K.

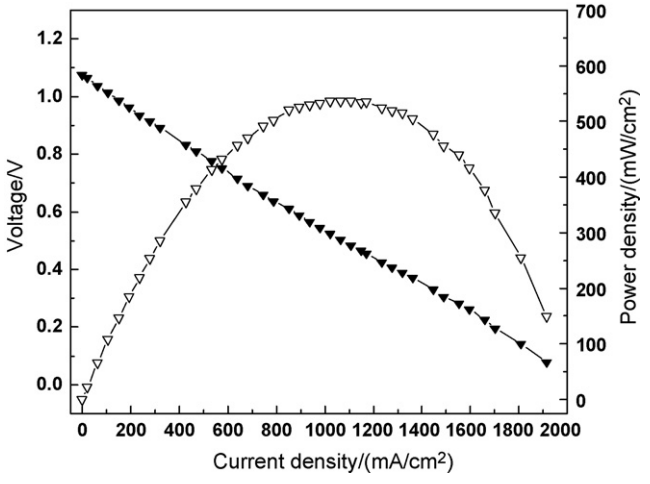

Fig. 8. Power density and current density–voltage relationships for cell-12 using a 10 wt.% CeO_2–25 wt.% Ni anode in H_2 at 1073 K.

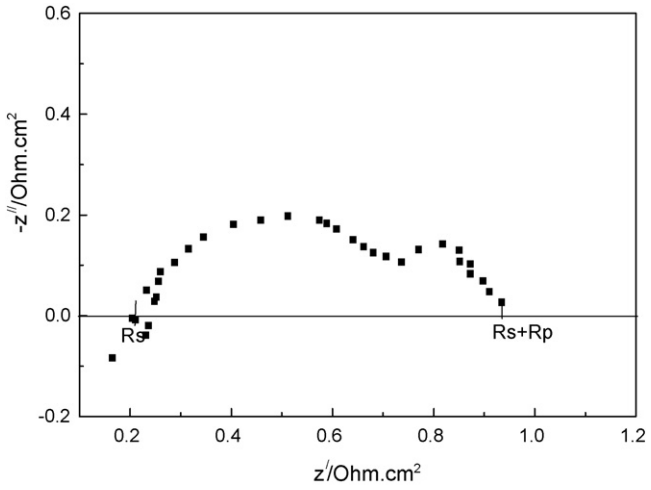

Fig. 9. Impedance spectra obtained with cell-12 in H_2 at 1073 K.

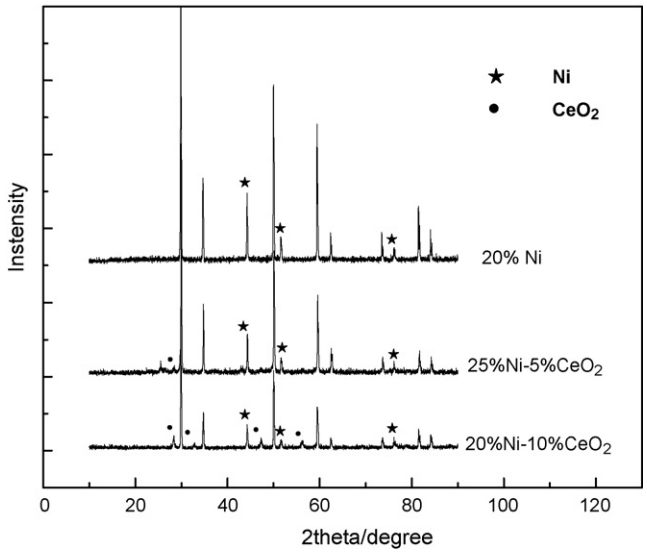

Fig. 10. X-ray diffraction patterns of reduced anodes.

framework. Fig. 11b is the surface micrograph for Ni/YSZ. The nickel on the YSZ surface is partially agglomerated. From cell-5, cell-8 and cell-11, we could conclude that 25 wt.% Ni content in the anode is necessary to ensure low ohmic resistance for these unit cells. On the basis of an essential Ni content, adding CeO_2 improved anode performance for the SOFC by changing the Ni dispersion on the YSZ. The ratio of Ni:CeO_2 needs to be investigated further.

3.3. Compared with TCC method preparing anodes

Two cells (cell-13 and cell-14) with anodes prepared by the TCC method were also tested in H_2 at 1073 K. These anodes and the p-YSZ/d-YSZ substrates were prepared by the same tape casting and firing procedures. The main characteristics of these two cells are listed in Table 2.

Table 2
Main characteristics of cell-13 and cell-14 in H_2 at 1073 K

	Anode porosity (vol.%)	Electrolyte thickness (μm)	Power density (mW cm^{-2})	OCV (V)
Cell-13	35	~28	143	0.971
Cell-14	40	~28	192	0.985

Table 2 reconfirms that cell performance was enhanced by increasing porosity of the anode, which has been investigated by other researchers [14]. Based on the data in Table 2 and Fig. 3, cell-3 with lower nickel content in the anode could be similar in power density to cell-14. Because nickel was dispersed on the surface on YSZ framework for anode obtained

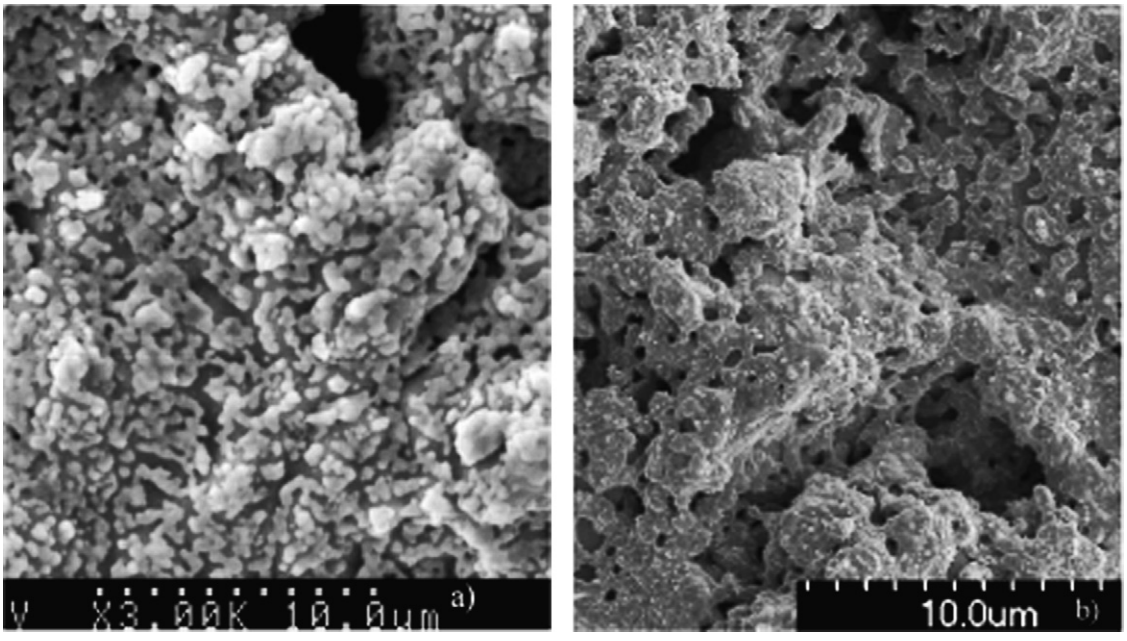

Fig. 11. SEM images for anodes prepared by impregnation: (a) Ni–CeO_2/YSZ and (b) Ni/YSZ.

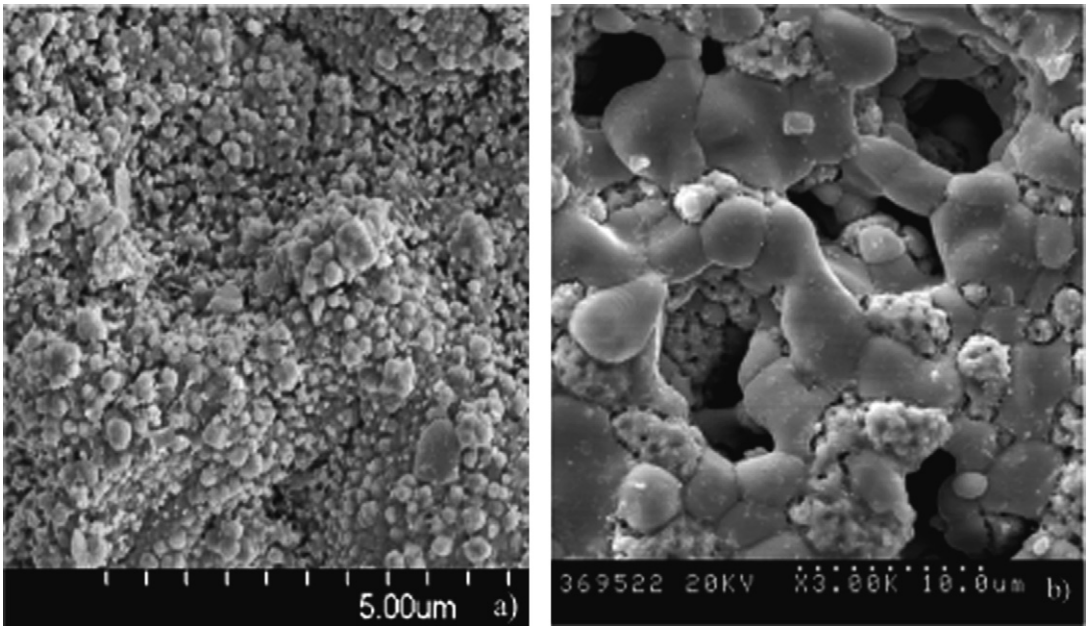

Fig. 12. SEM images for different anodes: (a) NiO/YSZ fabricated by impregnation and (b) Ni/YSZ prepared by tape casting and co-firing.

by TCI method and for the TCC method, nickel is located in middle of the YSZ framework (Fig. 12a and b). Fig. 12a shows nano-NiO formed on the YSZ surface, the particle size for most NiO grains to be about 100–200 nm. Conversely, the open circuit voltages (OCV) for cell-13 and cell-14 were 0.971 V and 0.985 V, respectively, and the OCV for cell-1–12 was about 1.05–1.09 V. This result indicated that it was easier to obtain dense YSZ electrolyte by co-firing p-YSZ/d-YSZ than NiO–YSZ/YSZ fabricated by co-firing at 1773 K for 6 h. Furthermore, large amounts of pore formers in the NiO/YSZ anode green tapes led to warping of NiO–YSZ/YSZ composite ceramic during the sintering process. However, the shrinkage of the p-YSZ/d-YSZ green tapes did not depend on the amount of pore formers. Thus, these green tapes could be co-fired without the resulting warpage. Although the impregnation steps are complex, tape casting p-YSZ/d-YSZ and a Ni impregnated anode is still a potential way for an anode supported SOFC.

4. Conclusion

Ni/YSZ and Ni–CeO_2/YSZ anodes were fabricated by tape casting and vacuum impregnation methods. Lower metal content was needed for these anodes, because nano-NiO was formed and reduced Ni or Ni–CeO_2 was dispersed on the surface of the YSZ. Twenty-five weight percent Ni was essential for these kinds of SOFC anodes to ensure low ohmic resistance. On this basis, doping CeO_2 into the Ni/YSZ anodes by mixed impregnation could improve cell performance through the decrease of cell polarization resistance. XRD patterns indicated that Ni and CeO_2 phases co-existed separately. XRD and SEM graphs showed additional CeO_2 enhanced Ni dispersion on the YSZ and increased the H_2 reaction activity of the anodes. With the 10 wt.% CeO_2–25 wt.% Ni/YSZ anode, the maximum power density was 530 mW cm^{-2} in H_2 at 1073 K. Finally, the OCVs for cells with these anodes were about 1.05–1.09 V, indicating fabrication preference for the p-YSZ/d-YSZ as compared to the co-fired NiO–YSZ/YSZ composite ceramic method. Impregnation is a complex process, but it is an important method for preparing a Ni-CeO_2/YSZ anode for an anode supported SOFC.

Acknowledgement

This work was financially supported by the National Nature Science Foundation of China (no. 90510006).

References

[1] S. Elangovan, J. Hartvigsen, A. Khandkar, et al., J. Power Sources 71 (1998) 354–360.
[2] A.M. Sukeshini, B. Habibzadeh, B.P. Becker, et al., J. Electrochem. Soc. 153 (4) (2006) A705–A715.
[3] Y. Nabae, I. Yamanaka, M. Hatano, et al., J. Electrochem. Soc. 153 (1) (2006) A140–A145.
[4] Y.J. Leng, S.H. Chan, S.P. Jiang, et al., Solid State Ionics 170 (2004) 9–15.
[5] W. Zhu, C.R. Xia, J. Fan, et al., J. Power Sources 160 (2006) 897–902.
[6] W.Z. Zhu, S.C. Deevi, Mater. Sci. Eng. 362 (2003) 228–239.
[7] A.C. Muller, D. Herbstritt, E. Ivers-Tiffee, Solid Sate Ionics 152–153 (2002) 537–542.
[8] S.K. Pratihar, A. Das Sharma, R.N. Basu, S.H. Maiti, J. Power Sources 129 (2004) 138–142.
[9] Y.J. Leng, S.H. Chan, K.A. Khor, et al., J. Power Source 117 (2003) 26–34.
[10] R.J. Gorte, J.M. Vohs, S. McIntosh, et al., Solid State Ionics 175 (2004) 1–6.
[11] S. Jung, C. Lu, H. He, et al., J. Power Sources 154 (2006) 42–50.
[12] S.-I. Lee, J.M. Vohs, R.J. Gorte, J. Electrochem. Soc. 151 (2004) 1319–1323.
[13] J. Kong, K. Sun, D. Zhou, Chin. J. Nonferr. Met. S3 (14) (2004) 380–383.
[14] F. Zhao, A.V. Virkar, J. Power Sources 141 (2005) 79–95.